Construction and Building Materials 468 (2025) 140291

Contents lists available at ScienceDirect

Construction and Building Materials

journal homepage: www.elsevier.com/locate/conbuildmat

Piezoresistivity assessment of self-sensing asphalt-based pavements with machine learning algorithm

Zhizhong Deng *, Quang Dieu Nguyen *, Aziz Hasan Mahmood *, Yu Pang, Tianxing Shi, Daichao Sheng *

School of Civil and Environmental Engineering, University of Technology Sydney, NSW 2007, Australia

ARTICLE INFO

Keywords:
Asphalt-based self-sensing sensors
Digital image correlation
Strain
Machine learning
Electrical resistivity
Percolation analysis
Predicted response

ABSTRACT

Due to its fast-curing process, asphalt binder has been increasingly used to replace conventional cementitious materials and to produce asphalt-based self-sensing sensors (ASS). The asphalt mixture does not require consideration of curing age, as asphalt-based samples can be cured at room temperature. This is because the asphalt binder transitions from a Newtonian liquid to a solid state upon cooling. The relationship between strain and electrical response is one of the factors that influences the self-sensing performance. In this study, four-electrode method was applied to ASS and 10 V of applied voltage was used to measure the piezoresistivity. The percolation thresholds of ASS, in the range of 0.5–1.0 wt%, was found based on study results. In order to analyse the strain of ASS, digital image correlation (DIC) method was applied, and the cyclic loading process was used to simulate the practical pavement situation. Furthermore, to enable the application of ASS and enhance the efficiency of the self-sensing system, a machine learning approach was applied in this study to establish the relationship between strain changes and the electrical response of ASS. The trained algorithm, exhibiting a high determination coefficient (reached 0.965), can be utilized to predict strain changes in self-sensing sensors based on fractional resistance changes. Artificial intelligence significantly enhanced the application potential of self-sensing sensors.

1. Introduction

Asphalt concrete composites are composed of cement, cationic emulsified bitumen, water, and fine aggregate fillers, forming an organic-inorganic material through the processes of cement hydration and asphalt demulsification [1,2]. While asphalt is prone to temperature variations and permanent deformations due to overuse, concrete pavements require extended curing times and joint installations to prevent cracking, which can result in a noisy driving experience. Combining these two materials into a composite addresses their respective drawbacks. Although cold mix asphalt is cost-effective, its lengthy curing process limits its application in heavy-duty pavements [3–5]. The cement in the composite enhances the mechanical properties of the pavement [6], however, its performance under traffic loads has not been thoroughly investigated. Significant advancements in asphalt concrete pavement are needed to align with the development of 'smart pavement' technologies [6–8]. The monitoring of the pavement health is to be taken into consideration.

Traditional asphalt material is insulation material [9], however, according to the previous study, with the help of conductive fillers, the enhancement of the conductivity of asphalt mixture has been successfully achieved [10]. The conductive asphalt specimen exhibits a strong electrical response to loading changes; however, the piezoresistivity response may weaken over time due to specimen deterioration [11–14]. One of the foundation materials of a smart pavement system is conductive filler [15–17], by adopting conductive fillers, including carbon fibres (CF) [10], carbon nanotubes (CNTs) [18], carbon black (CB) [19], etc., which affect the mechanical properties of the mixture besides changing conductivity to the composite. These fibrous fillers improve the conductivity of otherwise non/semi-conductive asphalt cement mixture and respond effectively to load change [20]. Previous research has shown that the sand volume and generated noise can affect the performance assessment of composites containing CF [21,22]. On the other hand, carbon black (CB) enhances the electrical conductivity and self-sensing capability of the mixture, while increasing the silica fume content further improves the composite's piezoresistivity [23].

* Corresponding authors.
E-mail addresses: zhizhong.deng@student.uts.edu.au (Z. Deng), quangdieu.nguyen@uts.edu.au (Q.D. Nguyen).

https://doi.org/10.1016/j.conbuildmat.2025.140291
Received 11 October 2024; Received in revised form 22 January 2025; Accepted 3 February 2025
Available online 18 February 2025

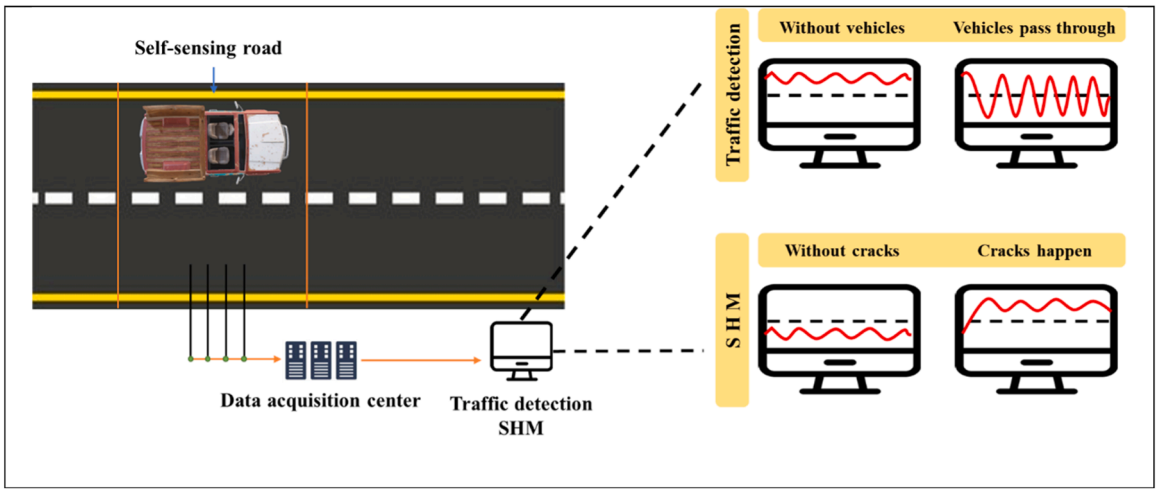

Fig. 1. Working method of self-sensing pavement.

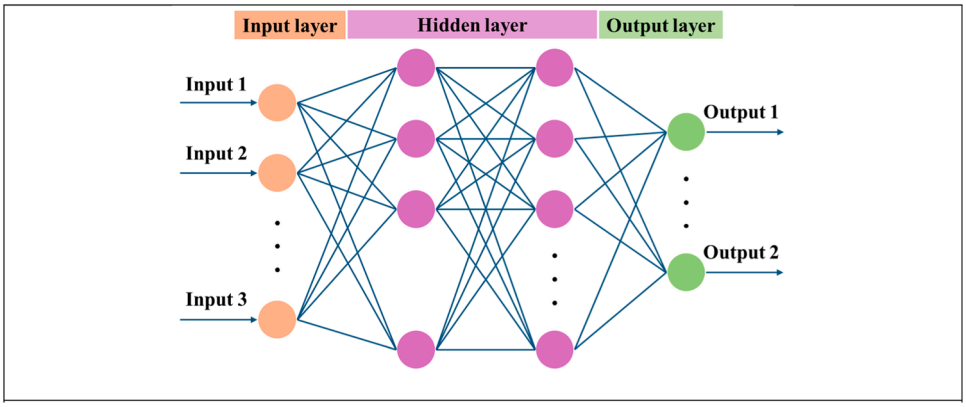

Fig. 2. The architecture of artificial neural network.

Table 2
The properties of the C450 bitumen, RTFO (Rolling thin film oven) (AS 2008-2013).

Bitumen Type	Viscosity at 135 ℃, PA.S	Flash point / ℃	Viscosity after RTFO treatment at 60 ℃, Pa.S	Mass change, percentage
C450	Max: 0.70	Min: 250	Min: 750; Max: 1300	−0.6 ~ 0.6

Table 1
Specifications of high temperature furnace.

Maximum Temp / ℃	Capacity / L	Temp Accuracy / ℃	Temp Fluctuation / ℃	Heating System
1200 ℃	216	1	±5 / ±3	Electric Element

Another functional filler material, carbon nanotubes (CNTs), can enhance the conductivity of specimens while also improving the compressive strength of the composite [24]. However, the sandwiched model design for CNTs predicts smoother agglomeration boundaries, which have minimal impact on the composites' mechanical properties while significantly enhancing their conductivity [25]. These conductive materials can help improve the mechanical properties of the composites. To address the durability and strength requirements of asphalt concrete pavement, this research selected carbon fibers (CFs) as the conductive filler to analyze the self-sensing capabilities of asphalt cement-based composites.

(a) (b)

Fig. 3. (a) Bitumen binder under normal status and (b) Furnace used to melt the asphalt binder.

The operational mechanism of self-sensing pavements is illustrated in Fig. 1, featuring a self-sensing system based on the piezoresistivity effect, as outlined in a previous research [26]. As the load changes, the

Table 3
Components of asphalt-based self-sensing specimens.

Sample type	Cylinder specimens							
CF wt%	0.5 %	1.0 %	1.5 %	2.0 %	2.5 %	3.0 %	3.5 %	4.0 %
Asphalt binder / g	71.82	71.82	71.82	71.82	71.82	71.82	71.82	71.82
Coarse aggregates / g	594	594	594	594	594	594	594	594
Fine aggregates / g	546	546	546	546	546	546	546	546

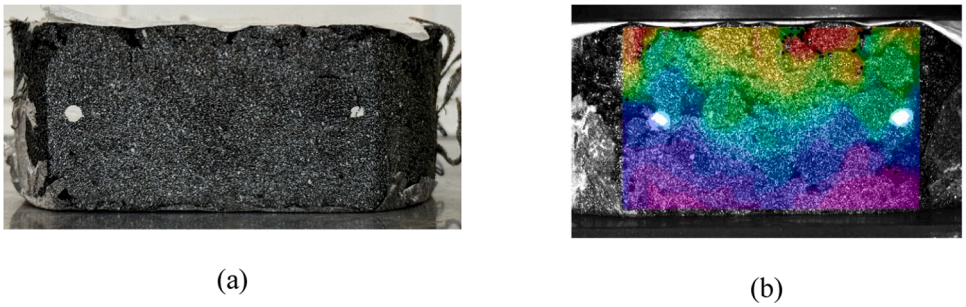

Fig. 4. (a)The asphalt based self-sensing specimen with scatter painting and (b) the DIC test result.

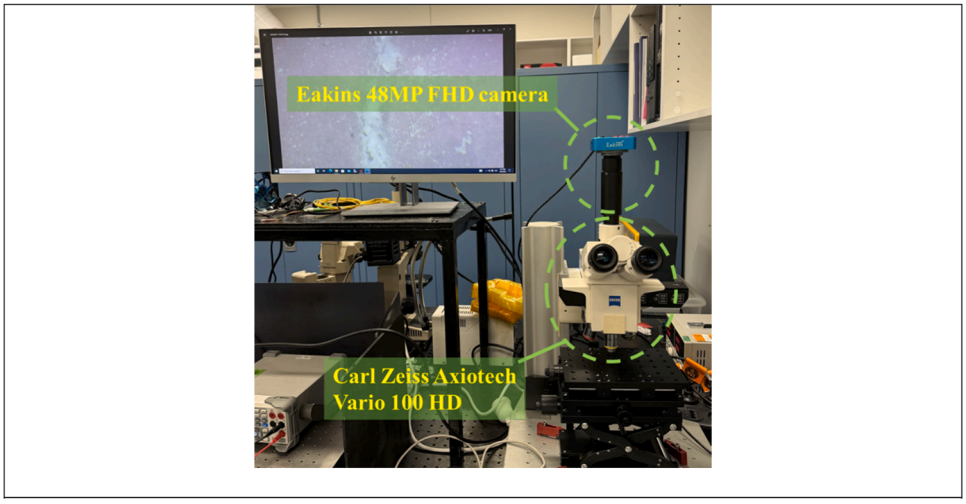

Fig. 5. The optical microscopic system.

resistance of the mixture simultaneously changes (from compacted distribution of fillers) as described by the fractional change in resistance (FCR) and the following equation:

$$FCR = \frac{R - R_0}{R_0} \times 100\% = \frac{\Delta R}{R_0} \times 100\% \quad (1)$$

where R in Eq. 1 is the resistance of the mixture after loading, and R_0 is the original electrical resistance of the unloaded specimen. The fractional change in resistance (FCR) offers a quantitative approach to analysing variations in the electrical resistance of the specimen.

This novel approach to assessing the pavement's electrical response to loads can be utilized to detect traffic flow, vehicle weight, and vehicle speed [27–29]. This functionality can assist in monitoring real-time traffic conditions and optimizing traffic management. Moreover, collected traffic data can be used to support the development of the weigh-in-motion system [30]. Cracks lead to change in resistance, as collected from the electrical signals to estimate the stress on the pavement and assess the level of damage to the pavement.

Previous studies on self-sensing asphalt-cement composites and smart pavements have predominantly focused on laboratory experiments, generating large amounts of data. The repetitive nature of the data makes it suitable for developing predictive models using machine learning (ML), a subset of artificial intelligence. Without considering rule-based algorithms and programming, ML can use specimens data to develop predictive models [31]. The use of ML in detecting concrete deterioration is not unheard. ML was used in corrosion area detection and evaluation, such as atmosphere corrosion [32], and pipeline corrosion [33]. Zhou et al. [34] applied ML to detect the micro-level damage to concrete beams. This has also been used in self-sensing technology. Roh et al. [35] made use of ML for the development of non-destructive evaluation of fibre-reinforced plastics.

By utilizing input training, machine learning (ML) can eliminate the need for theoretical modeling and expedite the decision-making process. An artificial neural network (ANN) can be trained using multiple sets of original data and corresponding targets to generate outputs that enhance machine learning (ML) performance. The schematic architecture of ANN is shown in Fig. 2. Previous study have investigated the application of ANN for reinforced concrete design [36]. The shear contribution of fiber-reinforced plastics in reinforced concrete infrastructures was analysed using an adaptive neuro-fuzzy inference system (ANFIS) [37]. Furthermore, machine learning was applied to Structural Health Monitoring, enhancing the detection system's

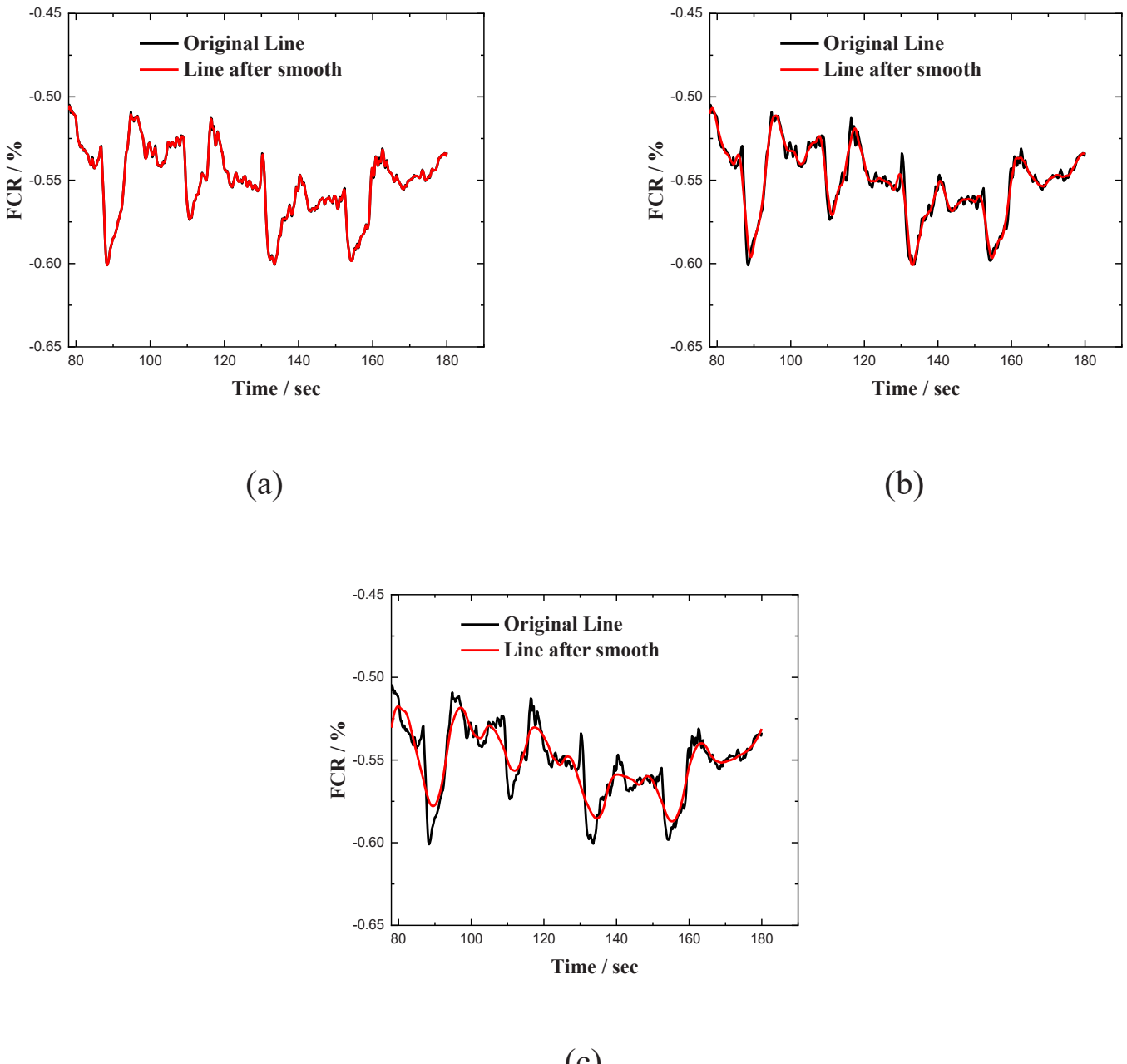

Fig. 6. Comparison of smoothing results when d= 3 and w is the variable (a) w= 5; (b) w= 25; (c) w= 65.

capability. However, limited research has analysed the application potential of ML in the self-sensing asphalt sensors for pavement detection. Specifically, the application of machine learning (ML) in asphalt mixtures incorporating self-sensing sensors with conductive additives has not been previously investigated. The experiment evaluated the piezoresistive response to loading changes and the mechanical properties of asphalt-based self-sensing mortar. The aim is investigating whether this mixture can be used in the practical situation. Furthermore, this study investigates the feasibility of self-sensing asphalt sensors by employing ML approach.

2. Materials and methodologies

2.1. Materials and mixture preparation

Class C450 level bitumen was chosen in this study and properties of this bitumen is shown in Table 2 based on AS 2008–2013. The normal status of bitumen was shown in Fig. 3(a). The test specimens combined coarse (nominal size of 10 mm) and fine (natural river sand) aggregates with asphalt as the binder. To establish conductive path in specimens, carbon fibre with an average diameter of 7 μm and length of 1 mm were added. To investigate the percolation thresholds of asphalt-based self-sensing sensors, eight dosages (0.5 %, 1.0 %, 1.5 %, 2.0 %, 2.5 %, 3.0 %, 3.5 %, and 4.0 %) of CF was chosen. The furnace (LABEC) used to melt the asphalt was shown in Fig. 3(b) and Table 1 summarised the asphalt-cement composites. Although capable of achieving a maximum temperature of 1200 °C, the furnace was operated at 175 °C as the highest viscosity of asphalt binder does not exceed 3 Pa·s at this temperature, making it suitable for mixing [38].

To enhance the electrical properties of asphalt concrete specimens, aligned carbon fibers (CF) should be uniformly dispersed within the asphalt matrix [39,40]. According to AS 2891, the melting temperature

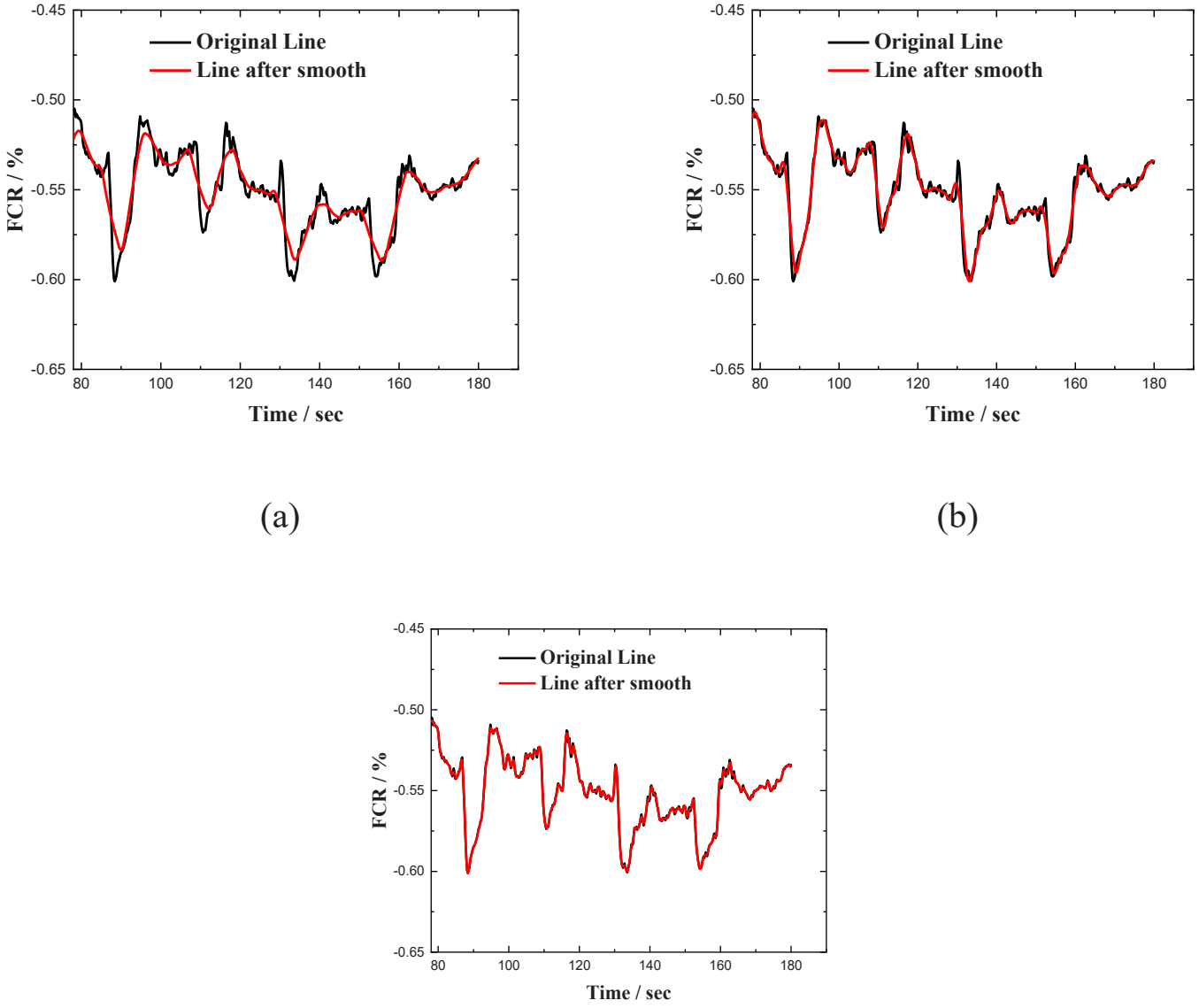

Fig. 7. Comparison of smoothing results when w= 25 and d is the variable (a) d= 1; (b) d= 3; (c) d= 5.

Table 4
The correlation coefficient and MSE results of different smoothed curves.

	W= 25, d= 5	W= 25, d= 3	W= 25, d= 1
Correlation Coefficient	0.99953	0.99915	0.97064
MSE	8.43303E−06	4.71244E−06	0.000289033

of the asphalt is 105 ± 5 ℃. In this experiment, the asphalt was melted at 175 ℃ for about two hours. At the same time, aggregates and CF were heated at the same temperature for the first two hours. Then, the CF and asphalt were mixed for about ten minutes for homogenous dispersion of the fibres. The mixture was then heated again at 175 ℃ for an additional two hours. Afterwards, aggregates were added to the asphalt-CF mixture and left into the furnace for an additional two hours heating which marked the final heating sequence for specimen preparation. At the end of heating, the mixture was ready to be poured into the moulds. In each mixing or moulding process, heating plate was applied to retain the temperature of the composites. Samples were de-moulded after 24 hours of initial curing in the moulds. The content of aligned CF in the samples ranged from 0.5 wt% to 4.0 wt% with an interval of 0.5 wt%, as summarised in Table 3, resulting in eight distinct dosages of CF.

Previous research indicates that carbon fibers exhibit excellent thermal stability, capable of withstanding extremely high temperatures of up to 3000 °C in an inert environment [41]. However, exposure to extreme temperatures above 2000°C can lead to graphitization [42]. Additionally, carbon fibers are prone to oxidation and degradation when subjected to temperatures in the range of 400–600°C [43].

In this study, the maximum temperature applied to melt the asphalt was only 175°C. Therefore, the influence of temperature on the carbon fiber's properties was not considered or investigated in this work.

2.2. Strain change evaluation

The strain of the asphalt-based self-sensing (ASS) specimen was

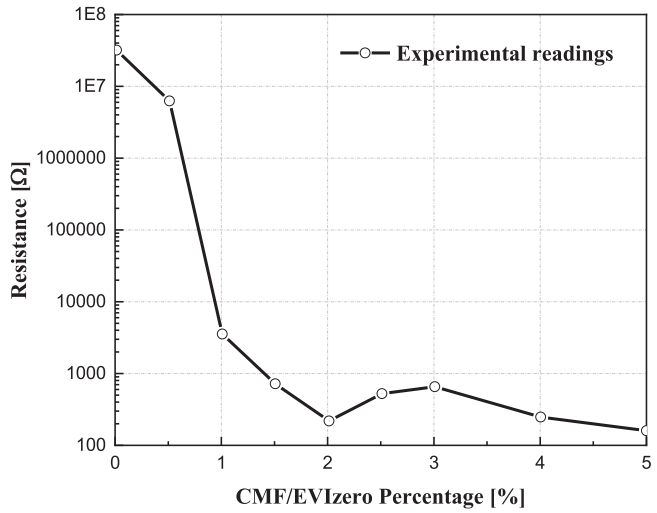

Fig. 8. Percolation thresholds of EVIzero-based self-sensing sensors [54].

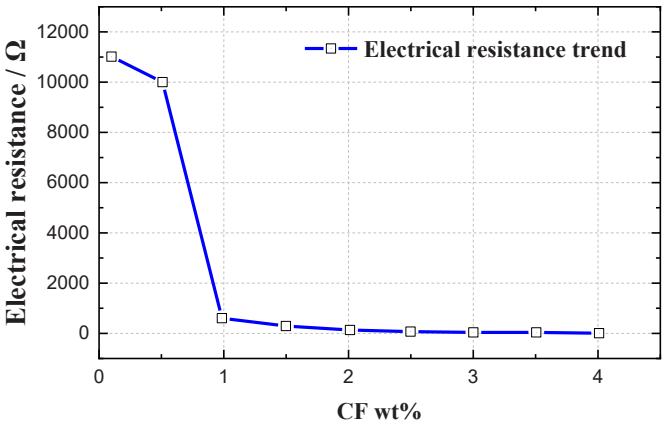

Fig. 9. Percolation thresholds of self-sensing asphalt-based sensors.

measured using the digital image correlation (DIC) method. The asphalt cylinder was ground to create a smooth, uniform surface. Then spray-paint was applied to the surface to present white colour spots for DIC test as shown in Fig. 4(a) and Fig. 4(b) showed the DIC test results. The DIC system was used to collect strain data. To ensure complete surface coverage and eliminate shadow interference, the camera and samples were aligned at the same horizontal level. [44]. The compressive strength of ASS specimens was tested by a universal testing machine under compression.

2.3. Electrical performance evaluation

2.3.1. Electrical resistivity

The electrical resistance of asphalt-based self-sensing specimens was measured, focusing specifically on their stress-electrical and strain-electrical resistance responses. Compressive stress was applied using a loading machine (AGX 50 kN), while electrical resistance was simultaneously measured with two multimeters under constant voltage and a four-electrode setup. The four-electrode method was employed as it can eliminate the effects of contact resistance between electrodes and asphalt [45]. Although two electrodes method have been applied in previous research for electrical resistance measurement due to an easier operation process [10,13], more reliable data can be recorded by using the four electrodes method. Moreover, the electrical resistance measured in this study can reflect the dispersion efficiency of the conductive fillers utilized.

The DC current was used in this study instead of AC current. Although AC current can reduce the polarization effects, there are several benefits that DC current can provide. As the carbon fiber added into the composites, the electrical resistance of asphalt mixtures was reduced. For the self-sensing test, the aim of self-sensing test was to measure the change of electrical resistance [46]. With DC current, the resistive components can be measured directly, but the capacitance and inductance of specimens should be considered if the study used AC current. The DC current measurement can provide a steady-state measurement [47]. It can make the correlation between resistance change with stress or strain easier. However, with AC current, the impedance analyser and frequency-dependent devices were required to separate resistive and reactive components. Without accurate control, the AC current may lead to inaccurate results. AC current can create a time-varying signal which requires careful phase and frequency analysis to isolate resistance changes, and this can lead to less intuitive strain sensing. For the short-term test, with proper experimental setup, the polarization effect can be minimized and cause little effect on experimental results [48]. In this study, each test for self-sensing specimens was only 2–3 minutes. Furthermore, with 175 ℃ melting temperature, the free ions content in asphalt mixtures was low which also reduce the polarization effect.

In conclusion, DC current can provide more stable measurement process and accurate results. Also, DC current can make experimental setup process simpler and avoid the influence of further variables.

2.3.2. Piezoresistivity test method

The self-sensing performance of the specimens was evaluated under varying compressive stress cycles to analyse the fractional resistance change. The cyclic compression test was tested successfully and recommended to measure the piezoresistivity of self-sensing samples in previous research [49]. The load application setup followed the same procedure as detailed in Section 2.3.1. Multimeters were connected to the four ends of copper electrodes on asphalt-based self-sensing specimens and the data was collected in two flash drives. The specimens were tested under a single loading event and four loading-unloading cycles at the same stress amplitude.

2.4. Data smoothing method

The electrical response experimental results were inevitably influenced by noise. In order to remove the noise influences, signal analyse process was employed [46]. The Savitzky–Golay smoothing filter (SGF) [50] was applied in this study to smooth a series of equal space data points and using following equation:

$$g_i = \sum_{n=-n_L}^{n_R} c_n \times f_{i+n} \tag{2}$$

Where n_R and n_L represent the number of data points to the right and to the left; c_n is filter coefficients; f_i represent different data points and g_i represent the linear combination. The w, known as window size, represent the number of $n_L + n_R + 1$. For all $n_L + n_R + 1$ points, the polynomial degree is fitted as least-squares to generate the SCF, for each f_i data point. Then at i position, g_i was applied to be the value of the polynomial.

2.5. Machine learning modelling and evaluation

Testing asphalt-based self-sensing sensors generates a large dataset, which can be efficiently analysed using machine learning to reduce the time required for data processing. The intelligent model can process large datasets and continuously learn to adapt to new information. Furthermore, high computational, decrease the reliance of expertise, and pattern recognition are highly improved the working efficiency

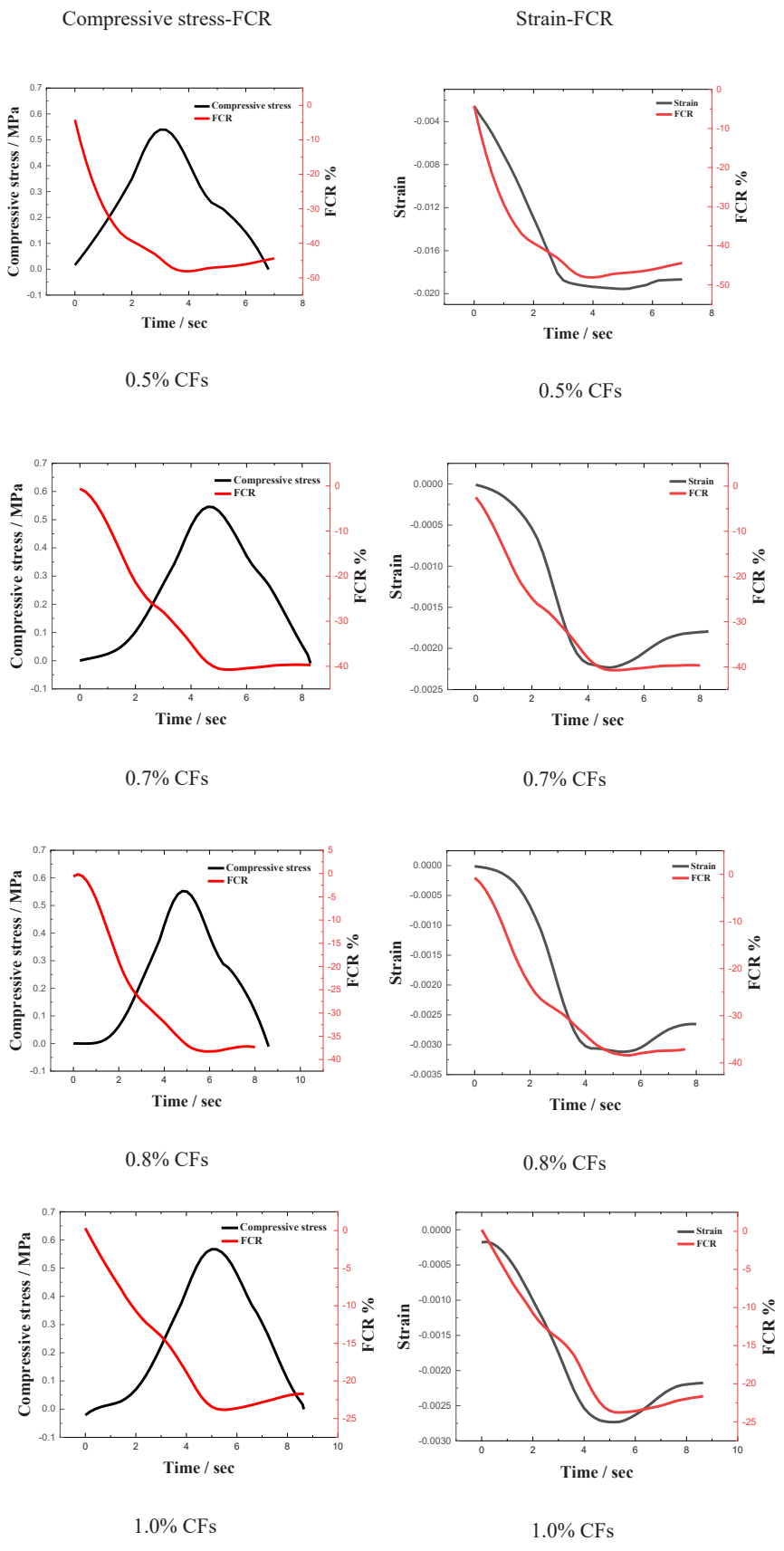

Fig. 10. Relationship of Fractional change in resistance (FCR) with compressive stress and strain in single load test.

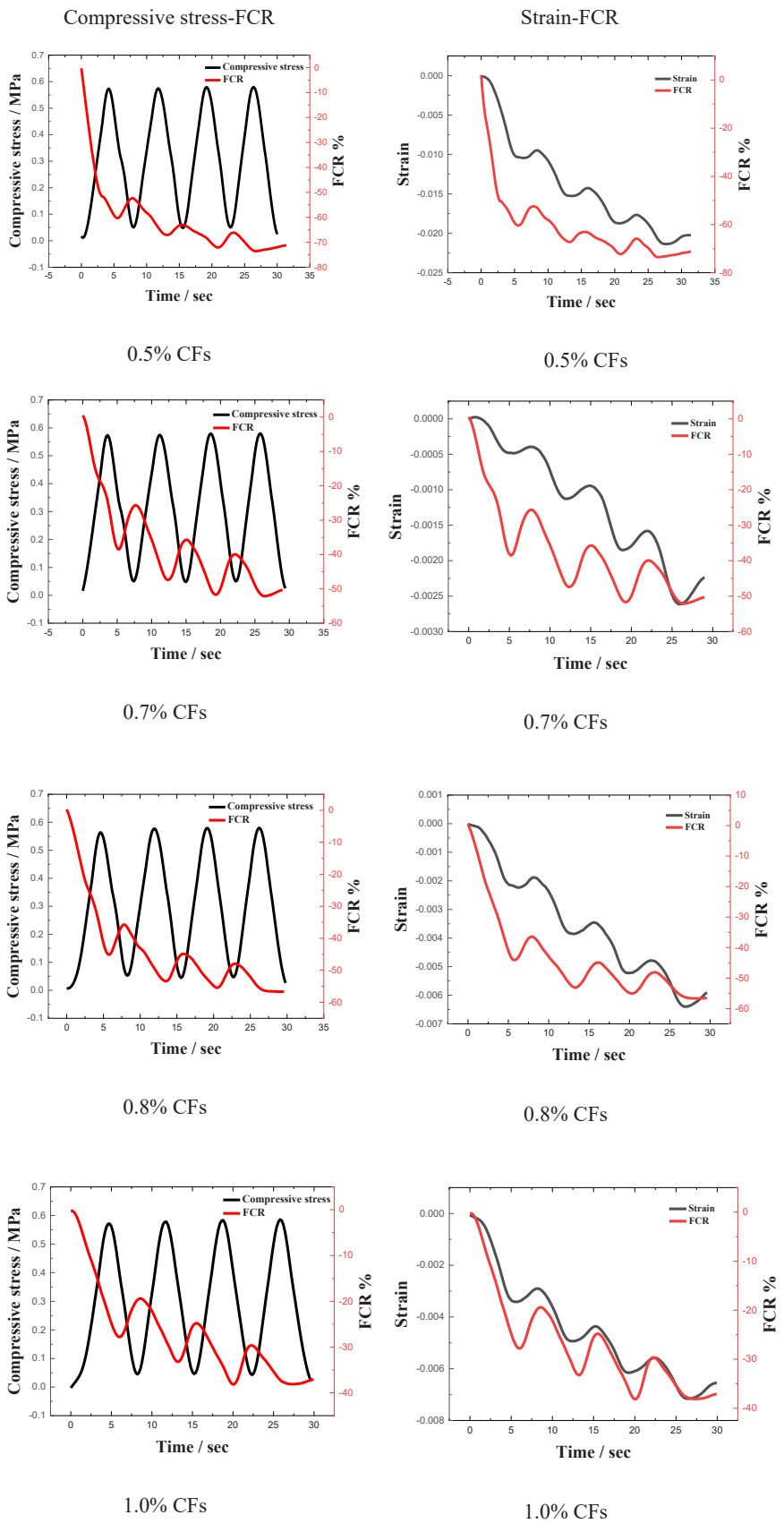

Fig. 11. Relationship of Fractional change in resistance (FCR) with compressive stress and strain in cyclic load test.

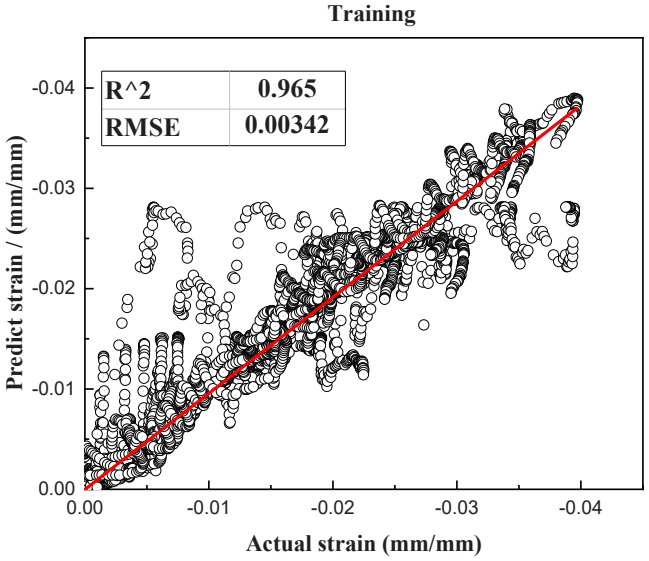

(a)

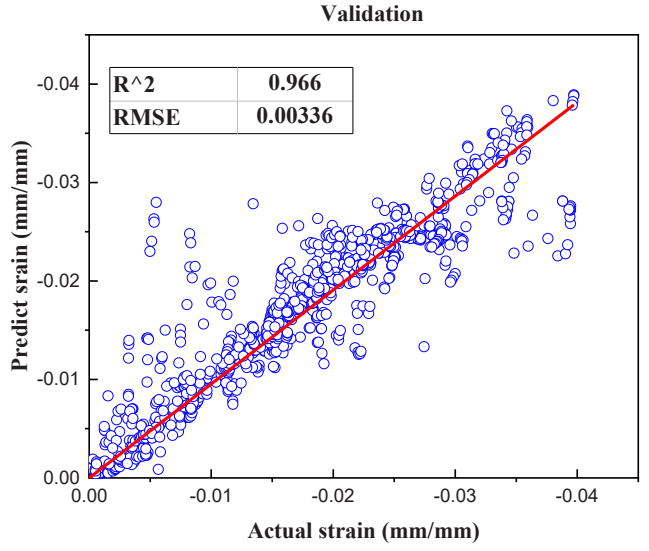

(b)

Fig. 12. Plot graphic of (a) training and (b) validation results of strain for whole dataset.

[51]. The trained artificial neural network (ANN) analysis system can generate outputs without being limited by whether the input data is known or unknown [35]. This approach can be beneficial for analysing the data gathered in this research. This study trained the artificial neural network (ANN) system using self-sensing performance test results. The selected inputs were the electrical response and the percentage of conductive filler content, while the output was the strain change of the samples. After training, the ANN algorithm consisted of cost function and input data. The cost value represents the errors between actual target value and model's predicted value. The cost function was used to calculate the sum of errors made by the model across all training examples. The ANN algorithm was used to minimise the cost value and improve the accuracy of the results. In this study, results were the strain

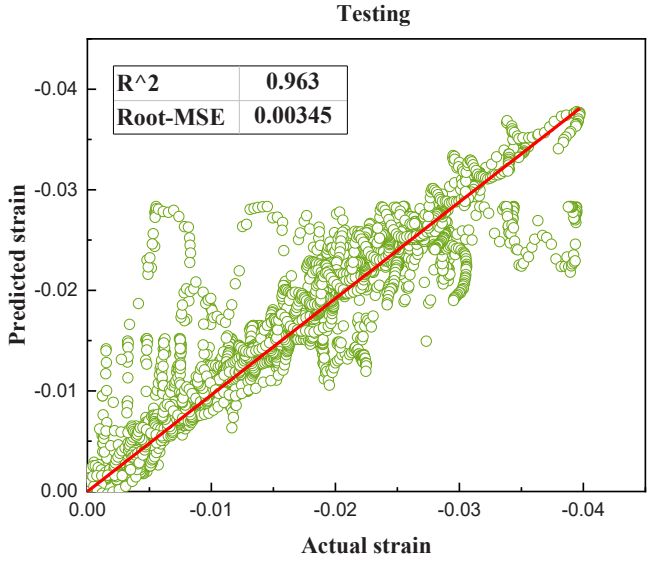

Fig. 13. The reliability testing of trained algorithm test results by extra datasets.

change, input value was fractional change of resistance (FCR) and percentage of carbon fiber contents. The primary objective of the ANN algorithm was to minimise the system's cost value and ensure that the final output value closely approximates the mean of the input data. Based on this principle, the piezoresistivity results of self-sensing specimens, conductive filler content, and strain change were used as input parameters for the ANN algorithm. The Levenberg-Marquardt algorithm was applied for ANN training and is shown in following Eqs. (3) and (4) [35]:

$$H = J^T J \tag{3}$$

$$g = J^T e \tag{4}$$

Eq. (3) represents Levenberg-Marquardt algorithm second-order training speed without calculating Hessian matrix. Eq. (4) presents the calculation method of gradient where J represent the Jacobian matrix and e represent the vector of network errors. In the Levenberg-Marquardt algorithm, Eqs. (3) and (4) are used as Newton-like update.

$$x_{k+1} = x_k - [J^T J + \mu I]^{-1} J^T e \tag{5}$$

Where μ represents scalar. With the decrease of μ, the success training number were increased. The Eq. (5) can become Newton's method when μ equal to zero. The equations from Eqs. (3) to (5) were utilised in Matlab Software. The inputs in this study are conductive filler content, FCR results, and the output is the strain of ASS samples. If filler content and FCR is not enough to conduct the algorithm, further parameters such as compressive strength will be added.

2.6. Optical microscope

This study analysed the micro-level holes in asphalt mixtures. The samples were compressed using a loading machine, and the compressive stress was maintained for five to ten minutes before being released. The compressed specimens were immediately scanned using an optical microscope. The optical microscope system was shown in Fig. 5. The type of microscope was a Carl Zeiss Axiotech Vario 100 HD, and the camera type was Eakins 48MP FHD.

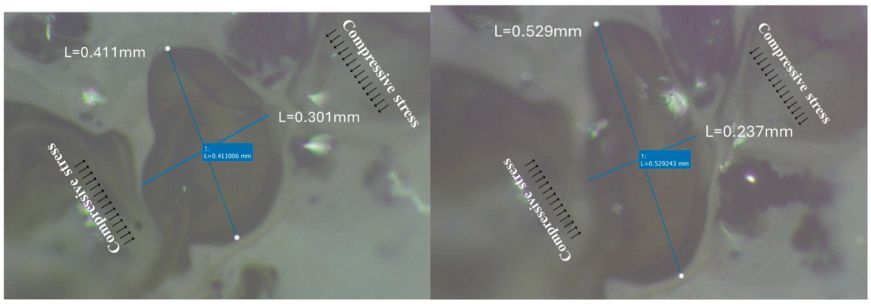

Fig. 14. Micro-level hole in asphalt-based self-sensing sensors before loading (left) and after loading (right).

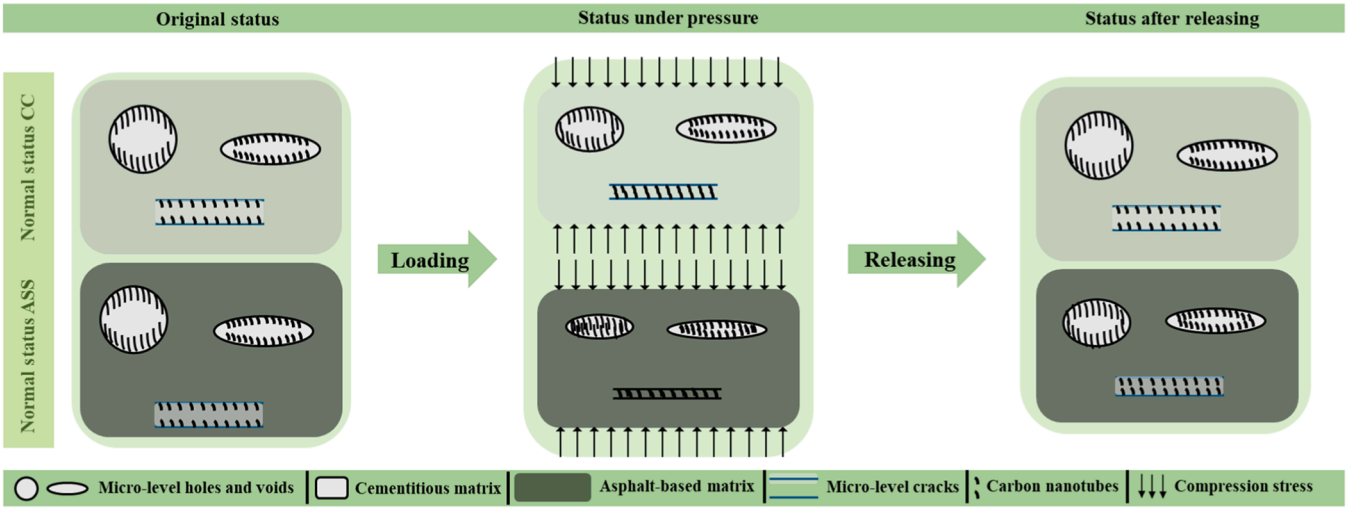

Fig. 15. Comparison of micro holes and micro-cracks change under compressive stress between cement-based samples (CC) and asphalt-based samples (ASS).

3. Results

3.1. Data smoothing results

The electrical response data was smoothed by Savitzky–Golay method as applied in previous study [52], as shown in Fig. 6. The smoothing process was influenced by window length, w and polynomial degree, d.

First, this study maintains the polynomial degree d at a low level while adjusting w to smooth the results. When $d = 3$, and $w = 5$, it is evident that the smoothing curve aligns perfectly with the original curve. The overfitting curve demonstrates that the smoothing process was not effective. In Fig. 6(b, c), the window length, w was progressively raised to 25 and 55. It is obvious that with the increase of w, the smoothing level has improved, but when the w value reached 65, the over smoothing problem was noticed while the curve under this w value can no longer represent the trend of the original curve. As such, for subsequent iterations, $w = 25$ was held constant while the polynomial degree, d was varied. The curve was over smoothed at $d = 1$ while the smoothing process was not effective at $d = 5$ which means it over fits the original trend without efficient noise reduction performance, as shown in Fig. 7. It can also be observed from the figure that at $d = 3$, the smoothing curve shows the best performance.

After calculating the mean squared error (MSE) and correlation coefficient for each smoothing curve, as shown in Table 4, it was observed that when w= 25 and d= 1, the correlation coefficient value was the lowest at 0.97064, with an MSE of 0.000289. The quantitative analysis indicates that d= 1 results in a weak correlation between the smoothed curve and the original curve. Under this condition, the curve was over-smoothed, as shown in Fig. 7(a). When d= 5, the smallest MSE value, as shown in Table 4, was achieved. However, with the highest correlation coefficient, the smoothed curve was overfitted to the initial curve, failing to effectively reduce noise influence. It can be observed from Fig. 7(c). Noticeably, when d= 3, the high correlation coefficient and low MSE demonstrated a strong correlation between the smoothed curve and the initial curve, without being overfitted or over-smoothed compared to other cases. It provides the best noise reduction performance while it did not change the initial trend of the curve, shown in Fig. 7(b).

Compared to previous study [52], although same d value has been chosen, a lower w value of 25 was applied in this study. Thus, the combination of w= 25 and d= 3 has been applied to each electrical response results in this study.

3.2. Percolation analysis

According to previous studies [53], analytical models have been used to evaluate percolation thresholds, which can be applied to asphalt composites. Furthermore, Birgin et al. [54] applied EVIzero, one of the substitutes of asphalt, to build self-sensing sensors with carbon fibres. The percolation of this novel material was evaluated based on the EVI-zero percentage, as shown in Fig. 8 [54]. A similar approach was adopted in this study to analyse the percolation thresholds of self-sensing asphalt-based sensors, with the findings presented in Fig. 9. The vertical axis represents the electrical resistance of the specimens, while the horizontal axis corresponds to the weight ratios of CF.

Based on analytical results, it can be observed that the critical volumetric fraction is at 1.0 % [55]. To analyse the reliability of this results, Birgin et al. [54] used experiments to confirm the percolation thresholds of EVIzero-based self-sensing sensors and found that the most

promising doping level was around 1 wt% carbon fibre content. In this study, the result demonstrated that, when carbon fibre content reached between 0.5~1.0 %, the self-sensing asphalt-based sensors can be in the transition area from being insulator to conductor. Comparing the results between this study and Birgin et al. [54], similar percolation thresholds results were shown in both experiments. In Birgin et al. [54], the experimental results proved that the analytical model method to search percolation thresholds does not provide an accurate results when analysing asphalt like materials. According to the study results, it can be concluded that 0.5–1.0 wt% carbon fibre contents stand out as the working area of ASS specimens.

3.3. Piezoresistivity

Fig. 10 presents the fractional change of electrical resistance (FCR) of asphalt-based self-sensing specimens. With the single loading process, the FCR rate keeps decreasing. The peak value of FCR rate of self-sensing specimens occurred when dynamic loads reached the highest value.

With the increasing content of functional fillers (CF), the FCR rate initially increased at the onset of the percolation threshold but decreased near its endpoint. This phenomenon has been observed in the results of previous studies [56]. Compared with stress-electrical results, the strain-electrical results showed a better relationship between self-sensing performance and strain change of specimens. The strain changes in the specimens influenced the electrical response during the loading process. Over time, the initial fractional change in electrical resistance for each loading cycle decreased compared to the previous one. For FCR rate in the whole loading process, the rate keeps decreasing which is different from the electrical response of the cement-based self-sensing specimens [57]. Based on Figs. 10 and 11, as the loading stress increases, the relationship between strain changes and electrical response becomes more apparent. During the single loading process, it is evident that the increase in FCR corresponds to the increase in strain. When the loading process ended, the strain change did not return to the initial state at the start of loading cycle, indicated temporary deformation. During this period, the FCR rate initially increased and then stabilized, corresponding to the strain changed. Previous study made a similar test to analyse the piezoresistivity performance of asphalt mixtures with electric arc furnace slag and graphene nanoplatelets which played the role of conductive fillers in the mixture [52]. Similar experimental results can be found from previous research [58]. However, compared to previous study [52], it solely illustrates the relationship between compressive stress and the electrical response of self-sensing asphalt-based samples. Without considering strain changes, the electrical response results become difficult to interpret. Due to the slow strain recovery process, the peak value of the FCR rate lagged the peak value of the compressive stress. Because of that, in the future research, strain-electrical response change of asphalt-based self-sensing specimens needs to be tested. According to the experimental results, ASS samples exhibit high sensitivity to changes in compressive stress, demonstrating significant potential for traffic detection and structural health monitoring applications in the future.

3.4. Predicted response from trained ML model

Using the training and testing data for the trained strain model discussed in Section 2.5, scatter plots illustrating the relationship between actual and predicted results are presented in Fig. 12. According to Fig. 12, the root mean squared errors (RMSEs) of the training and validation regression were 0.00342 and 0.00336 and it can be observed that the determination coefficients (R^2) were 0.965 and 0.966. The relationship between the actual strain and the predicted strain demonstrates a strong correlation. Based on the data from Matlab algorithm, the ML model which was trained by experimental datasets has great reliability. Compared to the previous study, the algorithm which applied in previous studies performed a lower R^2 value which was about 0.93 [54]. In this study, the algorithm showed a high potential to be applied to traffic detection. Compared to previous research, earlier studies utilized learning algorithms to design detection systems and apply them to traffic detection [53]. However, for those algorithm, complex numerical model and calculation process should be applied for detection results [27]. Compared to those complex processes, machine learning (ML) simplified the analysis process while enhancing reliability. With ML methods, the artificial neural network can be trained by the datasets to come up with an algorithm. The ML approach is simpler than previous algorithm [53] improving the working efficiency.

To prove whether the algorithm from MATLAB is reliable or not, another dataset was tested from a separate asphalt-based self-sensing specimens' group with the same CF contents. As the sensitive area of ASS can be found from Fig. 6, the CF content of samples which have been used to do the second test was 0.5 %, 0.7 %, 0.8 %, and 1.0 %. Fig. 13 showed the testing phase results. Based on Fig. 13, the relationship between actual strain and predicted strain datasets presents a strong performance, demonstrated by the value R^2 of 0.963. The prediction process of algorithm may highly be influenced by the content of CFs, and this study only focuses on the asphalt-based self-sensing samples optimum range. Through additional dataset analysis, this algorithm was validated as reliable for detecting strain changes in asphalt materials by monitoring variations in electrical resistance data.

4. Discussions on self-sensing performance

The electrical properties of self-sensing specimens are influenced by several factors. One of the factors that most significantly influence the fractional change in resistance ratio is the strain of the material. Birgin et al. [54] introduced the novel material EVIzero and applied this material as the additive of asphalt. According to their results, the self-sensing specimen with 1 wt% conductive filler exhibited the best performance. When the strain ranged between 0 and 50 με, the peak value of FCR rate reached about 20 %. Further, Xue et al. [59] made use of epoxy resin as the major material to form self-sensing sensors. When the strain of the sample reached its peak, the FCR rate was approximately 0.4 %. However, in this study, with 0.8 % content self-sensing asphalt-based sensors, the FCR rate was around 55 % and the strain of sample was 0.6 %, under 0.6 MPa compressive stress. It can be observed that with asphalt, the electrical response has been improved. Although replacement materials of asphalt have been used, self-sensing asphalt sensors demonstrated superior performance compared to other substitutes, as shown in previous studies.

Based on Fig. 14, it is obvious that under the compressive stress, the micro hole inside of the specimen has a deformation. Under the same compressive stress condition, ASS samples showed a clear deformation. For this reason, more conductive fillers can connect, forming additional conductive paths during the loading period.

According to Fig. 10, the FCR rate change showed a higher value compared to previous studies [60]. Under lower compressive stress, the strain change of ASS specimens was higher than cement-based mixtures. Due to the large shape change during the loading process, the structure inside of asphalt-samples presented a greater change than cement-based specimens. Because of that, more new conductive paths can be formed. As conductive paths in self-sensing specimens form within micro-level holes and microcracks under applied loads, the change in electrical resistance of asphalt-based self-sensing specimens is higher than that of cement-based self-sensing sensors. In that case, FCR rate of ASS samples was increased. Fig. 15 is summarised to illustrate this phenomenon that asphalt-based self-sensing sensors has a better reaction to the cyclic loads. During the load releasing process, the electrical resistance of self-sensing cementitious matrix can recover to original value following the loading releasing progress [56]. This phenomenon was indicated by previous study [61]. But the ASS samples cannot revert to its original

form as efficient as cement-based sensors. Because of that, the conductive path in ASS which formed during loading process will be partly kept in the micro-holes until next loading. Combined with Fig. 10, the FCR value of ASS keeps increasing following the twelve loading cycles. As a result, the self-sensing performance of sensors can be enhanced by incorporating asphalt mixtures.

5. Conclusion

This study analysed the electrical performance of asphalt-based self-sensing sensors and employed a machine learning method to develop a predictive algorithm for traffic detection. With the help of four-electrode method, DIC, and artificial neural network analysis, the working efficiency of self-sensing function was investigated. The objective of this study is to identify the percolation thresholds of self-sensing asphalt sensors and apply this novel self-sensing sensor for pavement detection. Combining laboratory results and learning algorithm, the following conclusion can be listed:

(1) With the addition of carbon fibers, the electrical resistance of asphalt-based samples has been decreased. The optimised working range of CF contents for ASS was found between 0.5 and 1.0 wt%.
(2) Due to the higher shape change of asphalt-based matrix, the form of conductive paths has been improved during loading process. As the conductive fillers have more chance to connect with each other, the piezoresistivity of asphalt-based self-sensing sensors has been enhanced. Thus, asphalt mixtures can improve the electrical response of self-sensing sensors.
(3) The trained algorithm using ML showed a great performance with the R^2 value higher than 0.96, it can be used to predict the strain change of asphalt-based matrix. This result demonstrates the potential of machine learning for enhancing self-sensing functionality.
(4) Based on experimental results and the machine learning method, this study demonstrates that the working efficiency of the self-sensing function can be enhanced using ML. With the help of machine learning, self-sensing sensors in asphalt-based matrix can be more functional in practical applications. In the future, more studies should be designed to enhance the cooperation of machine learning and self-sensing methods.
(5) Given that this study has demonstrated the potential of ML to enhance the operational efficiency of self-sensing systems, subsequent research will be directed towards the optimization of installation procedures, refinement of data acquisition processes, and mitigation of the environmental impact of self-sensing sensors, thereby advancing the methodology for their field application.

CRediT authorship contribution statement

Shi Tianxing: Writing – review & editing, Investigation. **Sheng Daichao:** Writing – review & editing, Supervision, Project administration, Investigation, Funding acquisition, Conceptualization. **Deng Zhizhong:** Writing – original draft, Visualization, Software, Resources, Methodology, Investigation, Formal analysis, Data curation, Conceptualization. **Nguyen Quang Dieu:** Writing – review & editing, Resources, Methodology, Investigation, Formal analysis, Conceptualization. **Mahmood Aziz Hasan:** Writing – review & editing, Methodology, Investigation. **Pang Yu:** Writing – review & editing, Investigation.

Declaration of Competing Interest

The authors declare that they have no known competing financial interests or personal relationships that could have appeared to influence the work reported in this paper.

Acknowledgements

The authors appreciate the Australian Research Council (ARC), Australia (IH180100010) and University of Technology Sydney Research Academic Program at Tech Lab (UTS RAPT).

Data availability

Data will be made available on request.

References

[1] W. Qiang, Y. Peiyu, A. Ruhan, Y. Jinbo, K. Xiangming, Strength mechanism of cement-asphalt mortar, J. Mater. Civ. Eng. 23 (9) (2011) 1353–1359, https://doi.org/10.1061/(asce)mt.1943-5533.0000301.
[2] Q. FU, K. ZHENG, Y. XIE, X. ZHOU, F. CAI, Fractal characteristic of pore volume of cement and asphalt mortar, J. Chin. Ceram. Soc. 41 (11) (2013) 1551–1557.
[3] D. Swiertz, P. Johannes, L. Tashman, H. Bahia, Evaluation of laboratory coating and compaction procedures for cold mix asphalt, Asph. Paving Technol. Proc. Assoc. Asph. Technol. 81 (2012) 81.
[4] T.A. Doyle, C. McNally, A. Gibney, A. Tabaković, Developing maturity methods for the assessment of cold-mix bituminous materials, Constr. Build. Mater. 38 (2013) 524–529, https://doi.org/10.1016/j.conbuildmat.2012.09.008.
[5] S. Al-Busaltan, H. Al Nageim, W. Atherton, G. Sharples, Mechanical properties of an upgrading cold-mix asphalt using waste materials, J. Mater. Civ. Eng. 24 (12) (2012) 1484–1491.
[6] I.N.A. Thanaya, S.E. Zoorob, J.P. Forth, A laboratory study on cold-mix, cold-lay emulsion mixtures, Proc. Inst. Civ. Eng. - Transp. 162 (1) (2009) 47–55, https://doi.org/10.1680/tran.2009.162.1.47.
[7] F. Moreno-Navarro, G.R. Iglesias, M.C. Rubio-Gámez, Encoded asphalt materials for the guidance of autonomous vehicles, Autom. Constr. 99 (2019) 109–113, https://doi.org/10.1016/j.autcon.2018.12.004.
[8] A.O. Monteiro, P.M.F.J. Costa, M. Oeser, P.B. Cachim, Dynamic sensing properties of a multifunctional cement composite with carbon black for traffic monitoring, Smart Mater. Struct. 29 (2) (2020), https://doi.org/10.1088/1361-665X/ab62e2.
[9] P. Leiva-Padilla, F. Moreno-Navarro, G. Iglesias, M.C. Rubio-Gamez, A review of the contribution of mechanomutable asphalt materials towards addressing the upcoming challenges of asphalt pavements, Infrastructures 5 (3) (2020), https://doi.org/10.3390/infrastructures5030023.
[10] P. Ahmedzade, B. Sengoz, Evaluation of steel slag coarse aggregate in hot mix asphalt concrete, J. Hazard Mater. 165 (1-3) (2009) 300–305, https://doi.org/10.1016/j.jhazmat.2008.09.105.
[11] S. Wu, L. Mo, Z. Shui, Z. Chen, Investigation of the conductivity of asphalt concrete containing conductive fillers, Carbon 43 (7) (2005) 1358–1363, https://doi.org/10.1016/j.carbon.2004.12.033.
[12] X. Liu, S. Wu, Research on the conductive asphalt concrete's piezoresistivity effect and its mechanism, Constr. Build. Mater. 23 (8) (2009) 2752–2756, https://doi.org/10.1016/j.conbuildmat.2009.03.006.
[13] X. Liu, S. Wu, N. Li, B. Gao, Self-monitoring application of asphalt concrete containing graphite and carbon fibers, J. Wuhan. Univ. Technol. Mater. Sci. Ed. 23 (2) (2008) 268–271, https://doi.org/10.1007/s11595-006-2268-2.
[14] X. Liu, S. Wu, Q. Ye, J. Qiu, B. Li, Properties evaluation of asphalt-based composites with graphite and mine powders, Constr. Build. Mater. 22 (3) (2008) 121–126, https://doi.org/10.1016/j.conbuildmat.2006.10.004.
[15] H.R. Rizvi, M.J. Khattak, M. Madani, A. Khattab, Piezoresistive response of conductive Hot Mix Asphalt mixtures modified with carbon nanofibers, Constr. Build. Mater. 106 (2016) 618–631, https://doi.org/10.1016/j.conbuildmat.2015.12.187.
[16] P. Apostolidis, X. Liu, A. Scarpas, C. Kasbergen, M.F.C. van de Ven, Advanced evaluation of asphalt mortar for induction healing purposes, Constr. Build. Mater. 126 (2016) 9–25, https://doi.org/10.1016/j.conbuildmat.2016.09.011.
[17] A.O. Monteiro, A. Loredo, P.M.F.J. Costa, M. Oeser, P.B. Cachim, A pressure-sensitive carbon black cement composite for traffic monitoring, Constr. Build. Mater. 154 (2017) 1079–1086, https://doi.org/10.1016/j.conbuildmat.2017.08.053.
[18] X. Liu, W. Liu, S. Wu, C. Wang, Effect of carbon fillers on electrical and road properties of conductive asphalt materials, Constr. Build. Mater. 68 (2014) 301–306, https://doi.org/10.1016/j.conbuildmat.2014.06.059.
[19] T. Schumacher, E.T. Thostenson, Development of structural carbon nanotube–based sensing composites for concrete structures, J. Intell. Mater. Syst. Struct. 25 (11) (2013) 1331–1339, https://doi.org/10.1177/1045389x13505252.
[20] S. Wu, P. Pan, M. Chen, Y. Zhang, Analysis of characteristics of electrically conductive asphalt concrete prepared by multiplex conductive materials, J. Mater. Civ. Eng. 25 (7) (2013) 871–879.
[21] F. Azhari, N. Banthia, Cement-based sensors with carbon fibers and carbon nanotubes for piezoresistive sensing, Cem. Concr. Compos. 34 (7) (2012) 866–873, https://doi.org/10.1016/j.cemconcomp.2012.04.007.
[22] A. Belli, A. Mobili, T. Bellezze, F. Tittarelli, P. Cachim, Evaluating the self-sensing ability of cement mortars manufactured with graphene nanoplatelets, virgin or recycled carbon fibers through piezoresistivity tests, Sustainability 10 (11) (2018), https://doi.org/10.3390/su10114013.

[23] H. Allam, F. Duplan, S. Amziane, Y. Burtschell, About the self-sensing behavior of smart concrete and its interaction with the carbon fiber percolation status, sand connectivity status and grain size distribution, Constr. Build. Mater. 324 (2022), https://doi.org/10.1016/j.conbuildmat.2022.126609.
[24] W. Dong, W. Li, Y. Guo, X. He, D. Sheng, Effects of silica fume on physicochemical properties and piezoresistivity of intelligent carbon black-cementitious composites, Constr. Build. Mater. 259 (2020), https://doi.org/10.1016/j.conbuildmat.2020.120399.
[25] W. Dong, Y. Guo, Z. Sun, Z. Tao, W. Li, Development of piezoresistive cement-based sensor using recycled waste glass cullets coated with carbon nanotubes, J. Clean. Prod. 314 (2021), https://doi.org/10.1016/j.jclepro.2021.127968.
[26] W. Dong, W. Li, Z. Luo, Y. Guo, K. Wang, Effect of layer-distributed carbon nanotube (CNT) on mechanical and piezoresistive performance of intelligent cement-based sensor, Nanotechnology 31 (50) (2020) 505503, https://doi.org/10.1088/1361-6528/abb503.
[27] W. Dong, W. Li, K. Vessalas, X. He, Z. Sun, D. Sheng, Piezoresistivity deterioration of smart graphene nanoplate/cement-based sensors subjected to sulphuric acid attack, Compos. Commun. 23 (2021), https://doi.org/10.1016/j.coco.2020.100563.
[28] Z.-Q. Shi, D. Chung, Carbon fiber-reinforced concrete for traffic monitoring and weighing in motion, Cem. Concr. Res. 29 (3) (1999) 435–439.
[29] B. Han, X. Yu, E. Kwon, A self-sensing carbon nanotube/cement composite for traffic monitoring, Nanotechnology 20 (44) (2009) 445501, https://doi.org/10.1088/0957-4484/20/44/445501.
[30] B. Han, K. Zhang, X. Yu, E. Kwon, J. Ou, Nickel particle-based self-sensing pavement for vehicle detection, Measurement 44 (9) (2011) 1645–1650, https://doi.org/10.1016/j.measurement.2011.06.014.
[31] H.B. Birgin, S. Laflamme, A. D'Alessandro, E. Garcia-Macias, F. Ubertini, A weigh-in-motion characterization algorithm for smart pavements based on conductive cementitious materials, Sensors 20 (3) (2020), https://doi.org/10.3390/s20030659.
[32] T.M. Mitchell, Machine Learning, Ed., McGraw-Hill, 1997.
[33] Y. Zhi, T. Yang, D. Fu, An improved deep forest model for forecast the outdoor atmospheric corrosion rate of low-alloy steels, J. Mater. Sci. Technol. 49 (2020) 202–210, https://doi.org/10.1016/j.jmst.2020.01.044.
[34] H. Ji, H. Ye, Machine learning prediction of corrosion rate of steel in carbonated cementitious mortars, Cem. Concr. Compos. 143 (2023), https://doi.org/10.1016/j.cemconcomp.2023.105256.
[35] K. Zhou, D. Lei, J. He, P. Zhang, P. Bai, F. Zhu, Real-time localization of micro-damage in concrete beams using DIC technology and wavelet packet analysis, Cem. Concr. Compos. 123 (2021), https://doi.org/10.1016/j.cemconcomp.2021.104198.
[36] H.D. Roh, D. Lee, I.Y. Lee, Y.-B. Park, Machine learning aided design of smart, self-sensing fiber-reinforced plastics, Compos. Part C Open Access 6 (2021), https://doi.org/10.1016/j.jcomc.2021.100186.
[37] O.R. Abuodeh, J.A. Abdalla, R.A. Hawileh, Prediction of shear strength and behavior of RC beams strengthened with externally bonded FRP sheets using machine learning techniques, Compos. Struct. 234 (2020), https://doi.org/10.1016/j.compstruct.2019.111698.
[38] H. Naderpour, S.A. Alavi, A proposed model to estimate shear contribution of FRP in strengthened RC beams in terms of adaptive neuro-fuzzy inference system, Compos. Struct. 170 (2017) 215–227, https://doi.org/10.1016/j.compstruct.2017.03.028.
[39] H. Wang, Z. You, J. Mills-Beale, P. Hao, Laboratory evaluation on high temperature viscosity and low temperature stiffness of asphalt binder with high percent scrap tire rubber, Constr. Build. Mater. 26 (1) (2012) 583–590.
[40] X. Zhang, et al., Piezoresistive characterization of polyethylene terephthalate–graphite composite, J. Test. Eval. 45 (1) (2017) 303–312, https://doi.org/10.1520/jte20160026.
[41] C. Zhang, Z. Liu, Y. Liu, Q. Cheng, C. Yang, L. Cai, Investigation of the mechanisms for stable superlubricity of poly(vinylphosphonic acid) (PVPA) coatings affected by lubricant, Friction 4 (4) (2016) 303–312, https://doi.org/10.1007/s40544-016-0117-7.
[42] J. Kinda, et al., Investigation of microscopic creep and shrinkage deformations of cement paste assisted by digital image correlation technique, Cem. Concr. Res. 166 (2023), https://doi.org/10.1016/j.cemconres.2023.107101.
[43] J. Xue, X. Wang, Z. Wang, S. Xu, H. Liu, Investigations on influencing factors of resistivity measurement for graphite tailings concrete, Cem. Concr. Compos. 123 (2021), https://doi.org/10.1016/j.cemconcomp.2021.104206.
[44] X. Wang, A. Al-Tabbaa, S.K. Haigh, Measurement techniques for self-sensing cementitious composites under flexure, Cem. Concr. Compos. 142 (2023), https://doi.org/10.1016/j.cemconcomp.2023.105215.
[45] B. Han, S. Ding, X. Yu, Intrinsic self-sensing concrete and structures: a review, Measurement 59 (2015) 110–128.
[46] M.U. Bromba, H. Ziegler, Application hints for Savitzky-Golay digital smoothing filters, Anal. Chem. 53 (11) (1981) 1583–1586.
[47] H.-W.-X. Li, G. Lyngdoh, N.M.A. Krishnan, S. Das, Machine learning guided design of microencapsulated phase change materials-incorporated concretes for enhanced freeze-thaw durability, Cem. Concr. Compos. 140 (2023), https://doi.org/10.1016/j.cemconcomp.2023.105090.
[48] F. Gulisano, T. Buasiri, F.R.A. Apaza, A. Cwirzen, J. Gallego, Piezoresistive behavior of electric arc furnace slag and graphene nanoplatelets asphalt mixtures for self-sensing pavements, Autom. Constr. 142 (2022) 104534.
[49] E. García-Macías, A. D'Alessandro, R. Castro-Triguero, D. Perez-Mira, F. Ubertini, Micromechanics modeling of the uniaxial strain-sensing property of carbon nanotube cement-matrix composites for SHM applications, Compos. Struct. 163 (2017) 195–215.
[50] H.B. Birgin, A. D'Alessandro, A. Corradini, S. Laflamme, F. Ubertini, Self-sensing asphalt composite with carbon microfibers for smart weigh-in-motion, Mater. Struct. 55 (5) (2022), https://doi.org/10.1617/s11527-022-01978-w.
[51] V. Kumar, A. Rawal, Tuning the electrical percolation threshold of polymer nanocomposites with rod-like nanofillers, Polymer 97 (2016) 295–299, https://doi.org/10.1016/j.polymer.2016.05.041.
[52] W. Dong, W. Li, L. Shen, S. Zhang, K. Vessalas, Integrated self-sensing and self-healing cementitious composite with microencapsulation of nano-carbon black and slaked lime, Mater. Lett. 282 (2021) 128834.
[53] S.-J. Lee, I. You, S. Kim, H.-O. Shin, D.-Y. Yoo, Self-sensing capacity of ultra-high-performance fiber-reinforced concrete containing conductive powders in tension, Cem. Concr. Compos. 125 (2022), https://doi.org/10.1016/j.cemconcomp.2021.104331.
[54] W. Li, et al., Development of self-sensing ultra-high-performance concrete using hybrid carbon black and carbon nanofibers, Cem. Concr. Compos. 148 (2024), https://doi.org/10.1016/j.cemconcomp.2024.105466.
[55] X. Xin, et al., Self-sensing behavior and mechanical properties of carbon nanotubes/epoxy resin composite for asphalt pavement strain monitoring, Constr. Build. Mater. 257 (2020), https://doi.org/10.1016/j.conbuildmat.2020.119404.